American Mineralogist, Volume 81, pages 982–994, 1996

Magma evolution recorded in plagioclase zoning in 1991 Pinatubo eruption products

KÉIKO HATTORI[1] AND HIROAKI SATO[2,*]

[1]Ottawa-Carleton Geoscience Centre, and Department of Geology, University of Ottawa, Ottawa K1N 6N5, Canada
[2]Department of Natural Environmental Sciences, Hiroshima University, Hiroshima 724, Japan

ABSTRACT

Plagioclase, the most abundant phenocryst at Mount Pinatubo, displays varying textures and compositions within the 1991 eruption products. In June 7–14 dome-forming andesite, plagioclase phenocrysts show prominent rims with higher MgO (0.04–0.06 wt%), $Fe_2O_3^T$ (0.6–0.8 wt%), and K_2O at given An than the interiors. The compositions of the rims are identical to those of microlites, which are abundant in the groundmass glass. White dacitic pumice, the most voluminous product of the June 15 eruption, contains partly corroded plagioclase phenocrysts but no prominent rims and no microlites. The interiors of phenocrysts from the dacitic pumice and the dome-forming andesite are remarkably similar in terms of textures and compositions. They show oscillatory zoning (mostly An_{35-60}), low MgO (<0.02 wt%) and $Fe_2O_3^T$ (0.10–0.30 wt%), and similar K_2O at given An. This similarity indicates that the two types of plagioclase phenocrysts formed in the same rhyolitic melt. The oscillatory zoning likely formed by temperature fluctuations in the convecting magma and incorporation and degassing of external fluids.

A portion of the felsic magma (~800 °C) mixed with a mafic melt (~1000–1100 °C) to become an andesitic magma that extruded to form the June 7–14 dome. All plagioclase phenocrysts in the andesite were derived from the felsic magma. The mixing caused destabilization of phenocrysts, forming sieve textures, dusty zones, and partial resorption. Extrusion of the mixed magma resulted in overgrowths on once-resorbed phenocrysts and the nucleation of plagioclase microlites in the groundmass glass. In the unmixed, remaining portion of the felsic magma, some plagioclase underwent partial resorption but did not develop overgrowths. This lack of overgrowths and the absence of microlites in the groundmass glass of the June 15 dacitic pumice indicate rapid magma ascent during the eruption and a short time span between the injection of a mafic melt and the cataclysmic eruption, supporting the linkage between the two.

INTRODUCTION

The Plinian eruption on June 15, 1991, from Mount Pinatubo, Philippines, released ~20 Mt (1 Mt = 10^{12} g) of SO_2 into the stratosphere, the largest release since satellite-based measurements started in 1978 (Bluth et al. 1992). The eruption ejected ~10000 Mt of pyroclastic material within 12 h (Scott et al. 1996), and this marks the eruption as the third largest in the twentieth century. Yet, the discharged magma is equivalent to <5% of a magma thought to be remaining beneath Mount Pinatubo after the eruption (Mori et al. 1993, 1996). The eruption products are predominantly (>99%) porphyritic, dacitic pumice (white pumice) with minor tan-gray phenocryst-poor pumice (gray pumice) and banded pumice, and minor fragments of dense andesite from the summit dome. The dome was first sighted in the crater on June 7, 1991 (Hoblitt et al. 1991; Bernard et al. 1996). It was a hybrid andesite formed from felsic and mafic magmas (Rutherford et al. 1993; Sato et al. 1993; Pallister et al. 1996), and it contained abundant rounded inclusions of basalt (~51 wt% SiO_2). The basalt fragments represent a mafic melt quenched during its injection into an overlying cool (~800 °C; Rutherford 1993; Hattori 1993) felsic magma reservoir, and the injection likely triggered the eruption of June 15 (Pallister et al. 1992).

Plagioclase is the dominant mineral in all eruption products, displaying various morphologies, complex fine-zoning patterns, textures, and compositions. Such zoning reflects the history of the parent magma. In this paper, we describe characteristic structures and zoning of the plagioclase, discuss evolution of the magma chamber, and evaluate the mode of mafic and felsic magma interaction at Pinatubo, which led to the cataclysmic eruption on June 15, 1991.

SAMPLES

Samples used for this study are representative specimens of white pumice, dome-forming andesite, and a basalt fragment in the andesite (Table 1). White pumice contains large phenocrysts and corresponds to the "crys-

* Present address: Department of Earth and Planetary Science, Kobe University, Kobe 657, Japan.

0003-004X/96/0708-0982$05.00

tal-rich pumice" (e.g., Westrich and Gerlach 1992) and "phenocryst-rich pumice" (e.g., Pallister et al. 1996) of other workers. The dacitic pumice sample was collected along the Sacobia River near the upper end of Clark Air Base. Large (<3 m) angular fragments of andesite, from the June 7–14 dome are abundant in the upper Maraunot Valley, and the andesite sample and the basalt inclusion were collected in the Valley, about 4 km west of the caldera wall, in August 1992. The eruption products were described by Bernard et al. (1996), Hattori (1993, 1996), Luhr and Melson (1996), Pallister et al. (1992, 1996), and Westrich and Gerlach (1992).

White pumice

The white pumice contains phenocrysts of plagioclase, hornblende rimmed by cummingtonite, biotite [X_{Mg} = molar ratios of $Mg^{2+}/(Mg^{2+} + Fe^{2+}) = 0.67–0.70$], quartz, unexsolved solid solutions of ulvöspinel-magnetite (magnetite) and ilmenite-hematite (ilmenite), anhydrite, and apatite. Microphenocrysts of olivine ($Fo_{80–83}$) rimmed by hornblende are common in some gray pumice but are not abundant in the white pumice. Chromite inclusions, common in the olivine, imply derivation from a mafic magma (Knittel et al. 1992).

Plagioclase phenocrysts, >40 vol% of the bulk rocks, are generally euhedral and 0.1–3 mm in length. Some phenocrysts are embayed and corroded owing to partial resorption (Fig. 1a). Angular fragments of plagioclase are common, and abrupt truncation of growth zoning indicates that much larger original crystals (Fig. 1a) were shattered during the ascent or eruption of the magma. Glass inclusions (<50 μm) are abundant, and fluid bubbles are common within the inclusions.

Plagioclase shows various degrees of interior corrosion within the phenocrysts (Figs. 1b and 1c), and arrays of minute fluid inclusions (<10 μm) are common along the boundaries between the corroded interiors and the outer calcic zones.

Dome-forming andesite

The andesite contains phenocrysts of plagioclase, hornblende, olivine ($Fo_{85–89}$) rimmed by hornblende, augite (X_{Mg} = 0.75–0.85), apatite, and oxides (magnetite and ilmenite). The olivine contains chromite inclusions, similar to olivine in dacitic pumice, and some hornblende grains are rimmed by cummingtonite. The dome-forming andesite contains anhydrite microphenocrysts, but they all have thin (~10 μm) reaction rims consisting of fine-grained calcsilicates (Hattori 1996).

Plagioclase phenocrysts (0.1–2 mm in length) are mostly euhedral (Figs. 2a and 2b), but there are angular fragments of once-larger euhedral crystals. Phenocrysts show dusty, patchy, and skeletal textures (Figs. 2b and 2c) with tubular to irregular glass inclusions (<100 μm) commonly containing fluid bubbles. In contrast to the white dacitic pumice, randomly oriented, euhedral microlites of plagioclase (10–50 μm wide and 50–150 μm long) are abundant in the groundmass glass.

TABLE 1. Bulk-rock compositions of samples

	White pumice		Dome-forming andesite	Basalt	
	Bulk	Matrix*	Bulk	Bulk	Matrix
			wt%		
SiO_2**	64.16	78.32	59.09	50.76	69.80
TiO_2**	0.49	0.14	0.64	0.89	0.30
Al_2O_3**	16.11	12.87	15.89	14.35	16.03
Fe_2O_3†	4.39	1.06	6.27	8.25	2.39
MnO**	0.10	0.04	0.12	0.16	0.13
MgO**	2.38	0.22	4.81	8.96	0.38
CaO**	4.84	1.21	7.11	10.08	2.26
Na_2O**	4.35	2.99	3.91	2.96	5.23
K_2O**	1.63	3.36	1.63	1.56	2.97
P_2O_5**	0.18	0.03	0.25	0.32	
LOI‡	1.42		0.10	0.40	
H_2O^+		0.31			
Sum	100.05	100.63	99.82	98.69	
			ppm		
Rb§	48	70	56	50	
Cs§	2.6		3.3	3.4	
Sr**	613	195	742	627	
Ba§	460	880	480	390	
Nb**	<5		<5	<5	
Zr**	113	85	104	94	
Y**	7		14	19	
Cr**	48		206	544	
Ni‖	8		27	62	
Zn‖	18		26	26	
Cu‖	16		26	65	
Co‖	31		26	25	
La§	16		20	24	
Sm§	2.5		3.9	5.4	
Th§	3.8		5.6	6.4	
U§	1.7		2	1.8	

* For major elements; weighted average of 21 spots of Westrich and Gerlach (1992) and 11 spots of Luhr and Melson (1996). For minor elements and H_2O determined by SIMS; Westrich and Gerlach (1992).
** Determined by XRF.
† Total Fe expressed as Fe_2O_3.
‡ Determined by heating 1 g at 1050 °C for 1 h.
§ Determined by INAA for bulk rock.
‖ Determined by ICP-AES.

Basalt

The basalt contains phenocrysts of olivine ($Fo_{86–88}$) rimmed by hornblende, augite (X_{Mg} = 0.78–0.85), and hornblende, and microphenocrysts of apatite and oxides. Plagioclase phenocrysts were not observed, but randomly oriented microlites of plagioclase (<100 μm wide and <500 μm long) constitute 30–40 vol% of the rocks. They show diktitaxitic and skeletal (fork-shaped) textures.

ANALYTICAL PROCEDURES

Plagioclase compositions were determined using a JEOL 733 Superprobe at Hiroshima University. The analytical conditions were as follows: 15 kV accelerating potential, ~20 nA current, with counting times of 40 s for major elements (Si, Al, Ti, Ca, Na, Mn) and 180 s for minor elements (Fe, Mg, K), and 5 μm beam diameter. Standards were synthetic wollastonite (Ca, Si), periclase (Mg), rutile (Ti), MnO (Mn), corundum (Al), adularia (K), albite (Na), and natural hematite (Fe). The absolute abundance of elements was obtained after correction of the X-ray intensities. Counting errors (one standard devia-

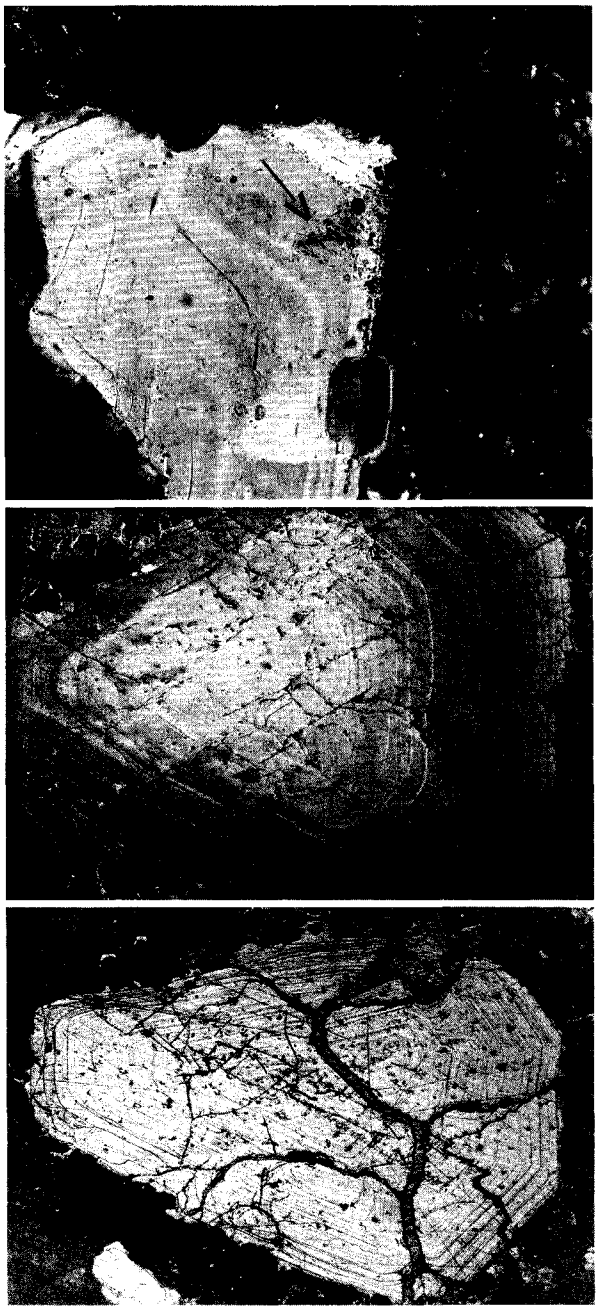

FIGURE 1. Photomicrographs of plagioclase phenocrysts in white dacitic pumice. (**a**) Corroded, broken fragment of plagioclase phenocryst. Melting started to occur in the phenocryst (arrow). Field of view = 1.0 mm. (**b** and **c**) Reflected-light Nomarski differential-interference-contrast photomicrograph after etching with HBF_4. Zones with higher Ca content are etched more deeply than those containing less Ca. Note rounded shapes, which are defined by outer Ca-rich zones. Field of view = 2.7 mm.

tion) of typical plagioclase analyses are as follows: 0.2 wt% SiO_2, 0.02 wt% TiO_2, 0.078 wt% Al_2O_3, 0.10 wt% CaO, 0.025 wt% MnO, 0.10 wt% Na_2O, 0.03 wt% $Fe_2O_3^T$, 0.008 wt% MgO, and 0.014 wt% K_2O. Detection limits, defined as 3σ of background values on both sides of X-ray peaks, are normally 0.025 wt% for $Fe_2O_3^T$, 0.008 wt% for MgO, and 0.01 wt% for K_2O.

The compositions of silicate minerals other than plagioclase were determined using a JEOL 6400 digital scanning electron microprobe at Ottawa-Carleton Geoscience Centre, equipped with a 40° take-off angle, 39 mm distance between the specimen and the counter, and a Link X-ray analyzer (EXL, LZ5). The analytical conditions were as follows: 20 kV accelerating potential, ~0.8 nA current on a Faraday cup, and 140–200 s counting time. Raw X-ray spectra were reduced to elemental concentrations using Link ZAF4-FLS. Standards were quartz (Si), phlogopite (K), wollastonite (Ca), $MnTiO_3$ (Mn and Ti), Fe_2O_3 (Fe), NiO (Ni), Cr_2O_3 (Cr), synthetic Al_2O_3 (Al), and MgO (Mg). Analyses are estimated to be accurate to 2% of the amount present, and detection limits are 0.1 wt%.

PLAGIOCLASE COMPOSITIONS

White dacitic pumice

Plagioclase phenocrysts show oscillatory zoning (Figs. 3a and 3c) with gradual outward changes from calcic to sodic compositions and sharp changes from sodic to calcic (Figs. 3b and 3c). The outer calcic zones commonly truncate inner growth zoning (Figs. 1b, 3a, and 3b), indicating partial resorption prior to growth of calcic zones.

The An contents vary widely from 30 to 80, mostly between 35 and 50, with consistently low MgO (<0.02 wt%) and $Fe_2O_3^T$ (0.012–0.22 wt%; Table 2; Figs. 3 and 4). The concentrations of MgO and $Fe_2O_3^T$ show no significant change from the interiors to the rims of the phenocrysts (Fig. 3), but a slight increase in $Fe_2O_3^T$ (<0.43 wt%) is observed in the margin of several crystals (Figs. 3b and 4). The K_2O concentrations, varying from 0.04 to 0.4 wt%, are inversely correlated with the content of An (Fig. 5).

Dome-forming andesite

Plagioclase phenocrysts show prominent calcic rims 10–30 μm wide (Figs. 2a and 2b). Along the boundary between the interior and the rim, dusty zones (up to 250 μm wide) containing numerous minute tubular glass inclusions are common, and the zones truncate inner growth zoning (Figs. 2b and 2c). The boundaries between rim and interior are sharp where no dusty zones are present (Fig. 2a).

The interiors of the phenocrysts have textures and compositions similar to those of the white dacitic pumice. They show oscillatory zoning with An_{30-64} (Fig. 6; Table 3), and calcic zones commonly truncate inner growth zones. The K_2O concentrations at a given An are identical to those from the white dacitic pumice (Figs. 5 and 7). The interiors are low in $Fe_2O_3^T$ (0.12–0.27 wt%; Figs. 2 and 6) and MgO (<0.007 wt%), but some grains contain up to 0.02 wt% MgO.

The rims contain high An_{50-73}, high $Fe_2O_3^T$ (0.60–0.80 wt%), and high MgO (0.05–0.07 wt%) (Fig. 6). Within the rims, An content decreases toward the outermost margins of the phenocrysts (Figs. 2a and 2b). The com-

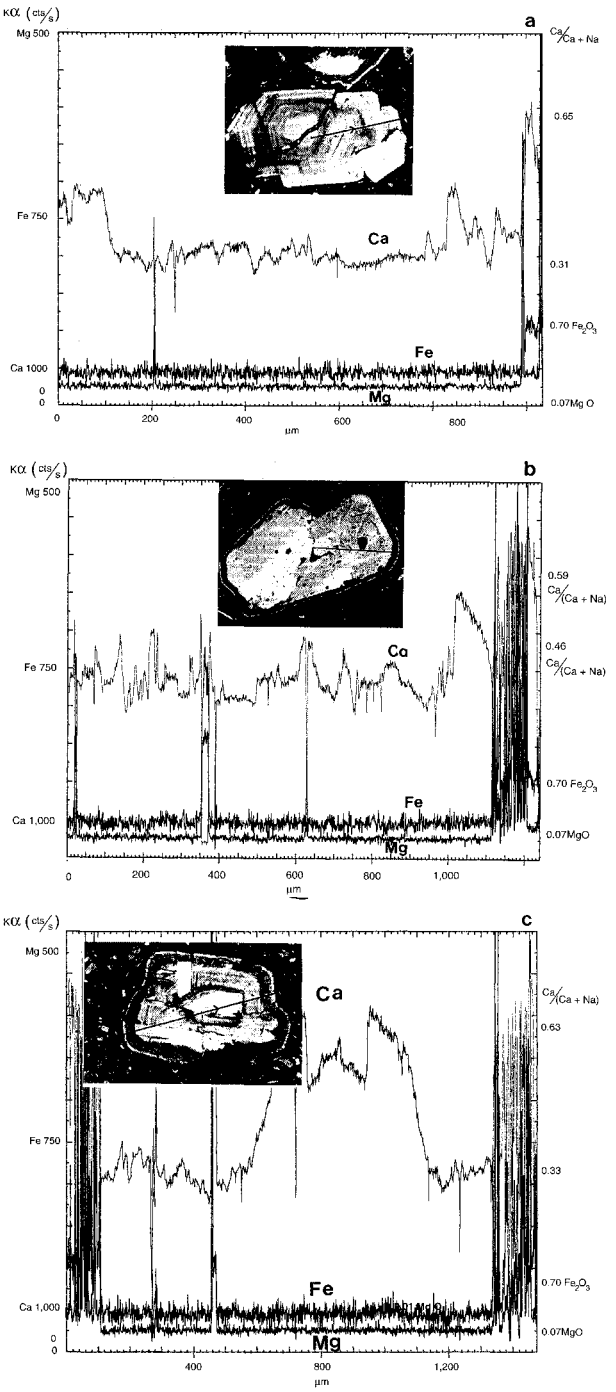

FIGURE 2. X-ray intensity variations of Ca$K\alpha$, Mg$K\alpha$, and Fe$K\alpha$ across three plagioclase phenocrysts from the dome-forming andesite with their photomicrographs under crossed polarizers. Numbers on y axes are counts per second recorded for Ca$K\alpha$, Fe$K\alpha$, and Mg$K\alpha$. The lines with arrows in the photomicrographs correspond to the line scans. The areas with highly variable concentrations of Ca, Fe, and Mg are dusty zones where minute tubal melt inclusions and remaining fine-grained, irregularly shaped plagioclase are intricately mixed. Analytical conditions: ~5 μm beam diameter, 15 kV accelerating potential, ~20 nA specimen current, and 5 s counting time. (**a**) Oscillatory zoning in the inner part with a calcic rim. (**b**) Dusty zone along the boundary between the inner part and rim. (**c**) Calcic zone in the interior (light) and reverse zoning at the rim.

→

positions of the rims are identical to those of the microlites in groundmass glass (Fig. 6), including the K_2O concentrations (Fig. 7). Their K_2O values at a given An are higher than those for the interiors of phenocrysts (Fig. 7).

Basalt

There are no plagioclase phenocrysts, probably reflecting high H_2O contents in the melt, but there are abundant microlites in the groundmass glass. The An contents of the microlites range from 46 to 65 (Fig. 8), and individual grains show Ca depletion toward their rims (Table 4). The concentrations of $Fe_2O_3^T$ range from 0.7 to 1.0 wt%, and those of MgO from 0.04 to 0.08 wt% (Fig. 8). The contents of K_2O in plagioclase are inversely correlated with An and plot along a steep trend on the K_2O vs. An diagram (Fig. 7); K_2O content at a given An is the highest in basalt microlites.

DISCUSSION

Crystallographic sites of Mg and Fe in plagioclase

The general formula of plagioclase is expressed as MT_4O_8, in which cations in T sites form tetrahedral nodes in the crystal. Cations in T sites are generally small and highly charged, whereas those in M sites are large. Plagioclase shows two maxima, corresponding to the M and T sites, on the "Onuma curve" (Onuma et al. 1968), which is defined by the ionic radii of cations and their respective crystal-melt partition coefficients [$D(i)$, defined as $i_{crystal}/i_{melt}$; Beattie et al. 1993]. Mg^{2+} is small and, together with Al^{3+}, is plotted on the curve for the T site. Similar D values for Mg^{2+}, Co^{2+}, and Zn^{2+} (Möller 1988), which have similar ionic radii and volumes, further confirm the crystallographic control of their siting in plagioclase.

In plagioclase, Fe may be present as Fe^{2+} and Fe^{3+}. The ionic radius of Fe^{3+} is similar to that of Al^{3+}, indicating its residence in the T sites (e.g., Smith and Brown 1988) and high $D(Fe^{3+})$. This is supported by the extensive substitution of Al^{3+} by Fe^{3+} in SiO_4^{4-} tetrahedra in melts (Dingwell et al. 1988; Mysen 1988). Fe^{2+} is much larger than Fe^{3+} but smaller than Ca^{2+} and Sr^{2+}, which makes entry into either the T or M sites difficult, but Fe^{2+} can occupy M sites because of its divalent charge. $D(Fe^{2+})$ is probably similar to $D(Mn^{2+})$ (0.05; Matsui et al. 1977) because the radii of the two cations are similar. $D(Mn^{2+})$ plots near the minimum of the Onuma curve (Jensen 1973).

Reflecting the change in Fe^{2+}/Fe^{3+} ratios in the melt, $D(\Sigma Fe)$, which is the sum of $D(Fe^{2+})$ and $D(Fe^{3+})$, varies as a function of f_{O_2} in the melt. High $D(Fe^{3+})$ in comparison with low $D(Fe^{2+})$ indicates that Fe in terrestrial plagioclase is predominantly Fe^{3+} (Smith and Brown 1988; Phinney 1992), and that Fe^{2+} may be significant only in

plagioclase formed from highly reduced Fe-rich magmas, such as lunar basalts (Longhi et al. 1976; McGee 1993). Accordingly, the concentrations of Fe in plagioclase in Pinatubo samples are reported as $Fe_2O_3^T$.

Diffusion of Mg and Fe in plagioclase

Cation charges are normally balanced in the crystal structure, which leads to the coupled substitution of $Al^{3+}Ca^{2+}$ by Na^+Si^{4+} or vice versa. This explains their extremely slow diffusion rates in plagioclase (Grove et al. 1984; Baschek and Johannes 1995) and the well-preserved, fine zoning of Ca/(Ca + Na) in volcanic plagioclase. Diffusion of Mg^{2+} and Fe^{3+} also requires a coupled cation substitution, such as $Mg^{2+}Si^{4+}$ by $Al^{3+}Al^{3+}$ and $Ca^{2+}Mg^{2+}$ by Na^+Al^{3+}. This implies very slow diffusion of Mg^{2+} and Fe^{3+}. Furthermore, Mg^{2+} and Fe^{3+} would not occupy adjacent T sites to maintain charge balance, which suggests high activation energy for their movement from one T site to a nonadjoining T site. We therefore consider the diffusion rates of Mg^{2+} and Fe^{3+} to be similar or even slower than those of Ca^{2+} and Al^{3+}, and volcanic plagioclase crystals probably retain their original compositional gradients and patterns for Mg^{2+} and Fe^{3+}.

Cation distribution coefficients between plagioclase and melts

The Ca/(Ca + Na) ratio of plagioclase is controlled by temperature, total pressure, melt-H_2O content, and Ca/(Ca + Na) ratio of the parent magma (Yoder et al. 1957; Kudo and Weill 1970; Drake 1976; Loomis 1979; Marsh et al. 1990; Housh and Luhr 1991). In particular, the H_2O content of a magma significantly affects the content of Ca^{2+} and Na^+ in plagioclase (Johannes 1978; Housh and Luhr 1991; Sisson and Grove 1993); plagioclase with higher An content crystallizes from a magma with higher H_2O content at a given temperature.

The experimental determinations of D(Mg) show a small decrease with decreasing temperature: ~0.068 ± 0.008 at 1250–1300 °C (Weill et al. 1980), 0.06 at 1250 °C (Blundy and Wood 1994), 0.065 at 1200^{+18}_{-11} °C (Longhi et al. 1976), ~0.05 at 1100–1200 °C (Sato 1989; Phinney 1992), and 0.021 ± 0.008 at 950–1050 °C (Sisson and Grove 1993). The value of 0.021 by Sisson and Grove (1993) is used in this study because their experimental conditions for an andesite system were similar to those for the studied samples.

The value of D(ΣFe) varies from 0.03 near the iron + wüstite buffer to 0.32–0.36 at 1200 °C under atmospheric

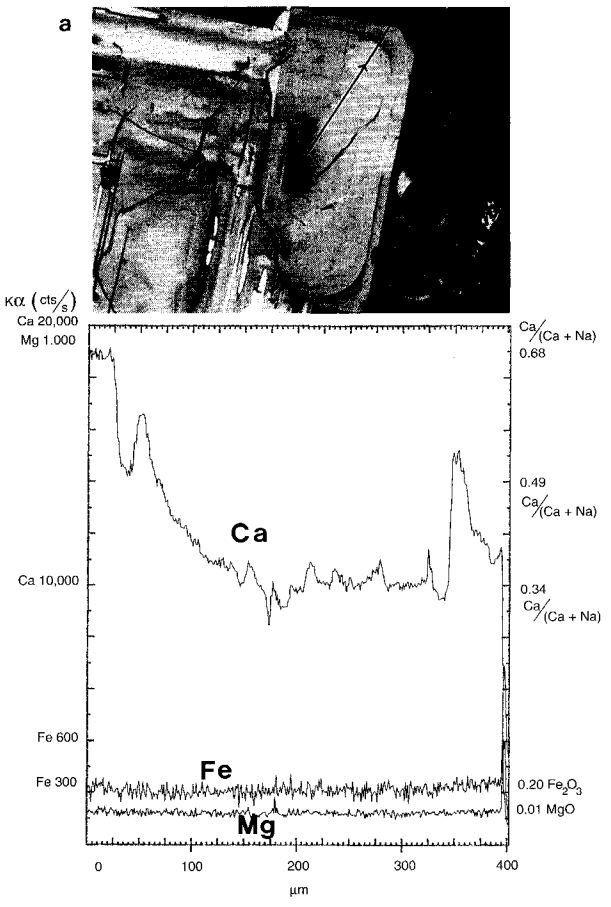

FIGURE 3 (above and right). X-ray intensity variations of Ca$K\alpha$, Fe$K\alpha$, and Mg$K\alpha$ across three plagioclase phenocrysts in the white dacitic pumice. Positions and directions of the line scans are shown in the photomicrographs. Numbers on y axes are counts per second recorded for Ca$K\alpha$, Fe$K\alpha$, and Mg$K\alpha$.

TABLE 2. Representative compositions of plagioclase in dacitic white pumice

Grain*	1-4C	1-2R	1-2C	1-2C	1-3R	2-3R	2-3R	2-3C	3-3C
Spot	14	22	23	24	37	45	46	47	92
SiO_2	50.87	58.48	58.83	54.83	57.20	58.84	54.21	58.87	46.79
TiO_2	0.026	<0.006	0.009	<0.006	<0.006	0.027	0.018	0.009	0.02
Al_2O_3	29.9	25.83	25.05	27.05	26.04	25.36	28.1	25.37	32.9
$Fe_2O_3^T$	0.14	0.26	0.21	0.17	0.24	0.18	0.32	0.21	0.22
MnO	<0.006	<0.006	0.011	0.028	<0.006	<0.006	0.012	<0.006	<0.006
MgO	<0.006	<0.006	<0.006	0.010	0.009	<0.006	0.021	<0.006	<0.006
CaO	13.56	8.16	7.14	9.93	8.78	7.19	11.2	7.54	16.38
Na_2O	3.52	6.53	7.36	5.76	6.25	7.10	4.96	6.91	2.33
K_2O	0.09	0.27	0.31	0.19	0.25	0.28	0.14	0.27	0.038
Sum	98.14	99.52	98.93	97.89	98.77	98.98	98.95	99.18	98.69
Ca/(Ca + Na)**	68.10	40.85	34.90	48.79	43.70	35.88	55.51	37.62	80.49

* C and R stand for interior and rim, respectively.
** Molar ratios.

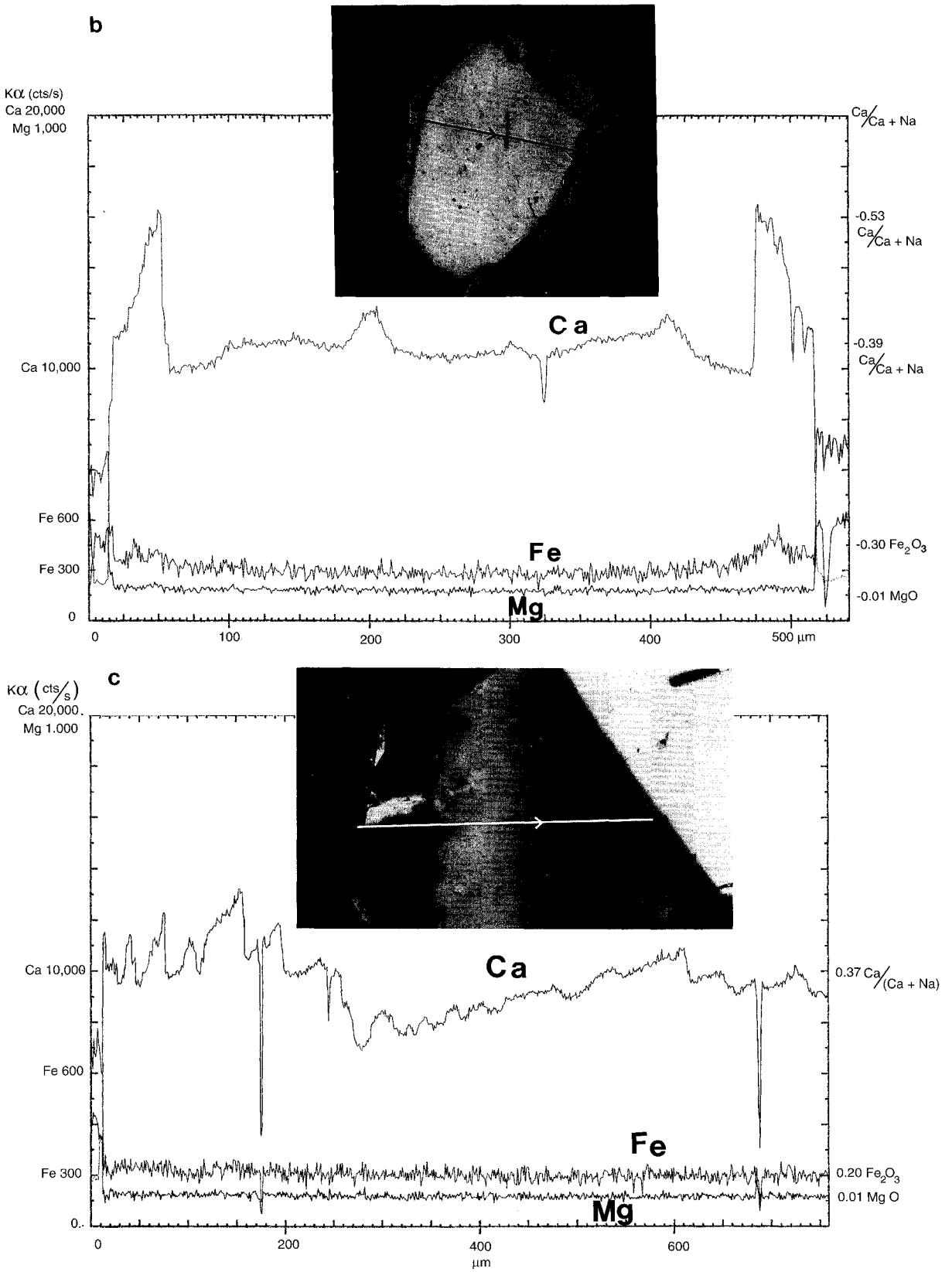

FIGURE 3. *Continued*

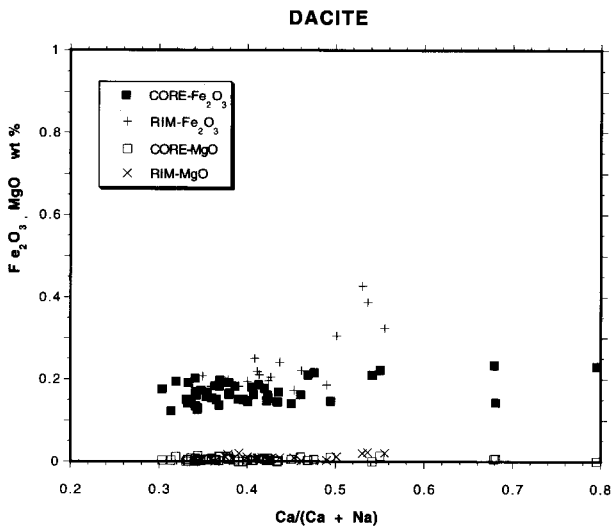

FIGURE 4. $Fe_2O_3^T$ and MgO vs. Ca/(Ca + Na) molar ratios of representative plagioclase phenocrysts in white dacitic pumice. Four to ten spot areas were analyzed for each grain.

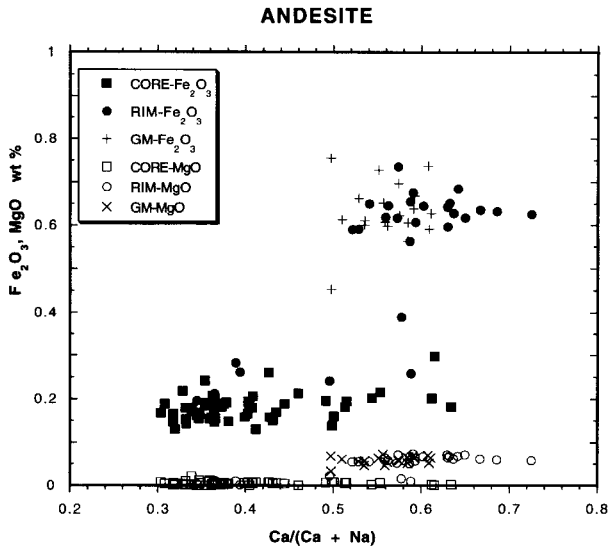

FIGURE 6. $Fe_2O_3^T$ and MgO vs. Ca/(Ca + Na) molar ratio of plagioclase in the dome-forming andesite. CORE-MgO, CORE-Fe_2O_3 = MgO and $Fe_2O_3^T$ concentrations in the interiors of plagioclase phenocrysts; RIM-MgO, RIM-Fe_2O_3 = MgO and $Fe_2O_3^T$ concentrations in the rims of plagioclase phenocrysts; GM-MgO, GM-Fe_2O_3 = MgO and $Fe_2O_3^T$ concentrations in plagioclase microlites in the groundmass glass.

conditions (Sato 1989; Phinney 1992). The former value, 0.03, corresponds to $D(Fe^{2+})$ because Fe is predominantly Fe^{2+} under the iron + wüstite buffer. $D(Fe^{3+})$ is calculated to be 0.35–0.4 using $D(\Sigma Fe)$ of 0.32–0.36 and the ratio of $Fe^{3+}/\Sigma Fe$ under atmospheric conditions. This is in good agreement with the value calculated from the experimental results of Sisson and Grove (1993) for an andesite system. Those authors obtained $D(\Sigma Fe)$ of 0.082 ± 0.017 at 950–1050 °C with the NNO buffer, where ~15% of the Fe in the melt is Fe^{3+}. This value of $D(\Sigma Fe)$ is translated into $D(Fe^{3+})$ of 0.43–0.66. We used $D(\Sigma Fe)$ of 0.25, which takes into account the high f_{O_2} of the Pinatubo magma, 3 log units above FMQ (Hattori 1993; Luhr and Melson 1996). The ratio of Fe^{3+}/Fe^{2+} in such a highly oxidizing melt is close to 1, following the method of Sack et al. (1980).

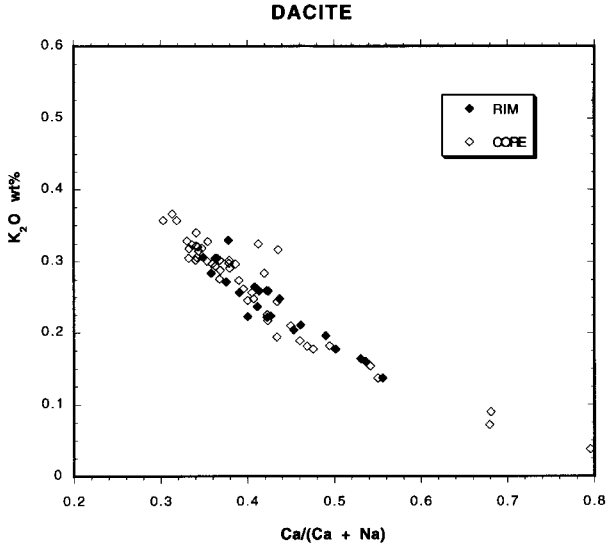

FIGURE 5. K_2O vs. An content of plagioclase in white dacitic pumice.

K_2O geothermometry

K^+ replaces Na^+ in the M site, which produces a reverse correlation between K_2O and Ca/(Ca + Na), as shown in Figures 5 and 7. The ratio of K/Na in the site is controlled not only by melt composition but also temperature. Plagioclase formed from a melt with higher K/Na shows higher K/Na at a given temperature. Within a given melt, plagioclase formed at higher temperatures incorporates more K^+, and it plots a steeper slope on a K_2O vs. An diagram (Sato 1984). The exchange reaction is expressed by Sato (1984); $\ln[(X_{Or}/X_{Ab}$ in magma)/$(X_{Or}/X_{Ab}$ in plag)] = $(8630 - 0.7T + 0.0053P - 4130X_{Ab}$ in plag)/RT, where R, P, and T are gas constant, pressure in bars, and temperature in kelvins, respectively, and X_{Or} and X_{Ab} are mole fractions of orthoclase and albite, respectively.

The bulk weight ratios of K/Na are comparable among basalt (~0.6), andesite (~0.5), and dacite (~0.4), and the ratio of the matrix glass in basalt (~0.6) is much lower than in the glass of dacite (~1; Table 1). High K_2O at a given An in basalt microlites cannot be attributed to high K/Na ratios of its melt. Instead, the variation in K_2O among samples reflects their temperatures of crystallization. The calculation using the groundmass composition (Table 1) yields the crystallization temperatures of 960–1140 °C for basalt microlites. The pressure correction is safely ignored for shallow magma reservoirs like that in

TABLE 3. Representative compositions of plagioclase in dome-forming andesite

Grain*	1-3B	1-3C	1-3C	1-3C	1-3R	1-5C	1-5R	1-15C	1-15C	1-15R	gm-7	gm-7
Spot	60	61	62	63	64	73	75	124	125	127	141	142
SiO_2	55.27	59.40	54.17	58.37	55.49	59.83	52.60	52.40	61.39	50.37	53.53	55.78
TiO_2	0.02	0.01	0.015	0.01	0.019	0.017	0.025	0.009	0.016	0.014	0.019	0.020
Al_2O_3	28.21	25.48	28.88	26.47	27.54	25.21	29.16	29.90	24.24	31.36	28.79	26.98
$Fe_2O_3^T$	0.18	0.20	0.22	0.26	0.59	0.18	0.65	0.18	0.17	0.63	0.56	0.76
MnO	0.014	0.022	0.031	0.014	0.019	<0.008	<0.008	<0.008	<0.008	0.028	<0.008	<0.008
MgO	<0.006	<0.006	<0.006	<0.007	0.055	<0.006	0.068	<0.006	<0.006	0.058	0.065	0.068
CaO	10.71	7.60	11.50	8.75	10.57	7.57	12.98	13.17	6.60	15.05	12.01	10.23
Na_2O	5.61	7.29	5.12	6.50	5.36	7.23	4.18	4.20	7.82	3.15	4.72	5.72
K_2O	0.18	0.29	0.15	0.24	0.24	0.29	0.16	0.10	0.34	0.11	0.19	0.28
Sum	100.19	100.28	100.07	100.60	99.88	100.31	99.82	99.96	100.56	100.76	99.87	99.82
Ca/(Ca + Na)**	51.34	36.55	55.38	42.66	52.15	36.65	63.18	63.41	31.81	72.53	58.44	49.72

* C and R stand for interior and rim, respectively. Grain numbers with "gm" refer to microlite grains in groundmass glass.
** Molar ratios.

the present case. The high end of the calculated temperatures is similar to the estimate, ~1200 °C, based on olivine-melt equilibria in basalt (Rutherford et al. 1993). The calculation for plagioclase phenocrysts from dacitic pumice yields 550–620 °C, using the average composition of the matrix glass (Table 1). The temperatures are much lower than the estimates (~780–800 °C) from the stability of cummingtonite (Rutherford 1993) and two-oxide thermometry (Hattori 1993). This discrepancy may be due to an overestimation of K_2O or an underestimation of Na_2O in the matrix glass used for the calculation because their concentrations show a wide variation. Pallister et al. (1996) noted much lower K_2O (average = 2.36 wt%; n = 23) and higher Na_2O (average = 3.47 wt%; n = 23) near plagioclase phenocrysts, and the calculation using their compositional data yields the temperature of 680–740 °C.

The rims of phenocrysts and microlites from the andesite plot between basalt microlites and plagioclase phenocrysts from dacitic pumice (Fig. 7), indicating their crystallization at a temperature cooler than that of the basalt microlites but hotter than that of the phenocrysts from dacite. Again this is consistent with the proposal that the dome-forming andesite was a mixed magma of cooler felsic and hotter mafic magmas.

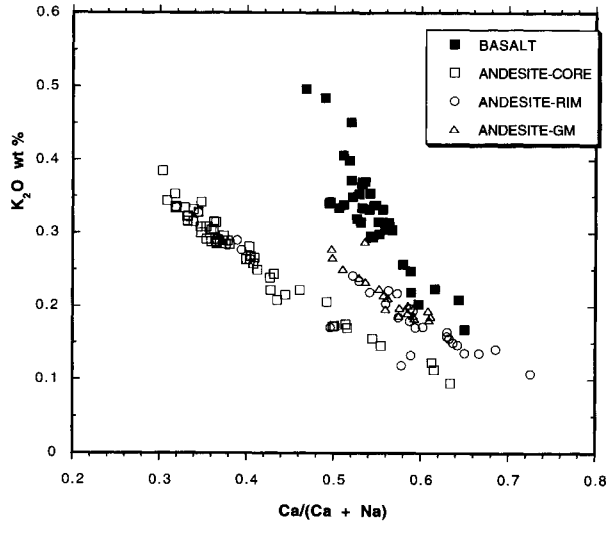

FIGURE 7. K_2O vs. An content of plagioclase phenocrysts and microlites in the dome-forming andesite and basalt. ANDESITE-GM = microlites in groundmass glass of andesite. Note that the compositions of the phenocryst rims are similar to those of microlites in the groundmass glass in andesite.

Mixing of magmas recorded in plagioclase

The interiors of plagioclase phenocrysts in the dome-forming andesite are very similar to those of the dacitic pumice in terms of texture, An content, the concentration of K_2O at given An, and the concentrations of MgO and $Fe_2O_3^T$. The resemblance of the two is remarkable considering the relationship between K_2O contents and An contents is different even among different eruption products from a single volcano (Sato 1984). In addition, MgO and Fe_2O_3 concentrations are much lower in the Pinatubo plagioclase than in plagioclase from many other volcanic rocks (Sato et al. 1993, and in preparation; Singer et al. 1995). For example, they are distinctly lower than those for the interiors of plagioclase phenocrysts from the dome-

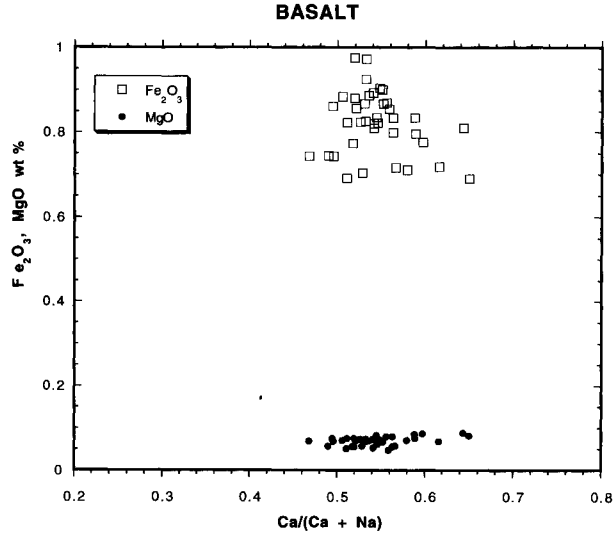

FIGURE 8. $Fe_2O_3^T$ and MgO vs. Ca/(Ca + Na) molar ratio of plagioclase in basalt.

TABLE 4. Representative compositions and mineral formula of plagioclase microlite in basalt

Grain*	1C	1R	5C	5R	11C	11R	2C
Spot	1	2	11	12	31	32	6004
SiO_2	51.35	52.69	51.90	54.22	54.62	55.24	54.48
TiO_2	<0.007	0.033	0.026	<0.007	0.033	0.036	0.028
Al_2O_3	29.95	28.93	29.49	27.93	27.19	27.01	27.81
$Fe_2O_3^T$	0.690	0.776	0.810	0.717	0.821	0.887	0.868
MnO	0.025	0.025	<0.008	<0.008	0.015	0.008	<0.006
MgO	0.082	0.087	0.089	0.058	0.062	0.070	0.066
CaO	13.36	12.39	12.97	11.38	10.90	10.60	10.95
Na_2O	3.98	4.62	3.97	4.82	5.01	5.08	5.36
K_2O	0.17	0.20	0.21	0.30	0.34	0.37	0.31
Sum	99.61	99.77	99.47	99.42	98.99	99.30	99.86
Ca/(Ca + Na)**	64.97	59.71	64.35	56.61	54.59	53.55	53.03

* C and R stand for interior and rim, respectively.
** Molar ratios.

forming andesite of Mount Unzen (Sato et al. 1993, and in preparation), although the bulk compositions of the andesites from Unzen and Pinatubo are very similar and both are hybrids of mafic and felsic magmas. This striking similarity between the two types of phenocrysts in Pinatubo indicates that the phenocrysts in the andesite and dacitic pumice were formed in a single magma reservoir.

To confirm the derivation of all plagioclase phenocrysts from a felsic magma, the compositions of relatively small phenocrysts were determined (Fig. 9). K_2O contents at a given An are identical to those of large phenocrysts, and the interiors have low MgO and $Fe_2O_3^T$. We could not detect any compositional signatures of a mafic melt in these small phenocrysts and conclude that all plagioclase phenocrysts in the andesite originated from the felsic magma. The MgO content of the parent melt for the plagioclase phenocrysts is calculated to be <0.5 wt%, and that of $Fe_2O_3^T$ ranges from 0.5 to 1.1 wt%, assuming f_{O_2} to be 3 log units above FMQ. The f_{O_2} represents the value shortly before eruption, and therefore the calculated value of $Fe_2O_3^T$ is the maximum estimate. Both concentrations correspond to a rhyolitic melt. The estimated MgO concentrations in melt are similar to those for groundmass glass in the dacitic pumice (Table 1) and for melt inclusions in phenocrysts (0.17–0.19 wt%; Westrich and Gerlach 1992). The concentrations of $Fe_2O_3^T$ are similar to those in groundmass glass (Table 1).

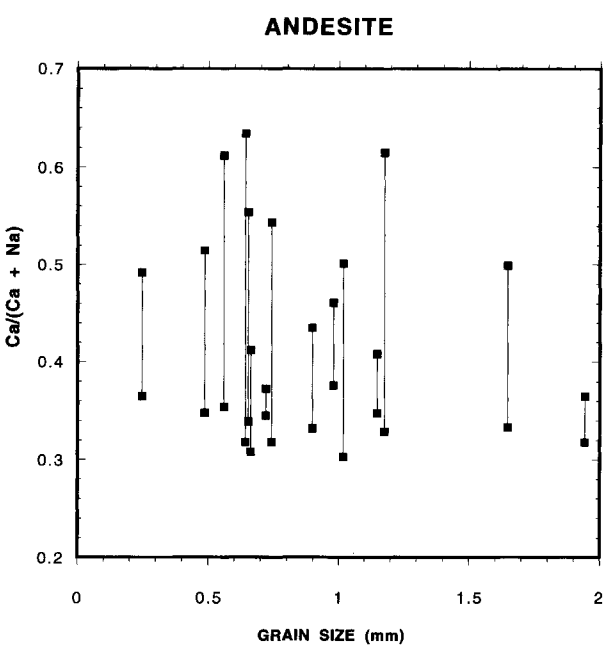

FIGURE 9. Ca/(Ca + Na) molar ratio vs. apparent size of each plagioclase phenocryst in the dome-forming andesite. The apparent size of each plagioclase phenocryst as observed in this section is expressed as the radius of a circle of equal area.

The Pinatubo magma in the preeruptive chamber has been referred to as a dacitic magma on the basis of bulk chemical compositions; however, the melt was rhyolitic throughout the crystallization of plagioclase phenocrysts. This does not necessarily imply that the dacitic magma is a rhyolitic melt containing xenocrystic ferromagnesian minerals. It is likely that the parent melt evolved from a mafic melt, but that the nucleation of plagioclase was retarded because of high melt-H_2O contents. Plagioclase crystallization started only after the melt became rhyolitic.

Inner growth zones are commonly truncated by dusty zones. Tsuchiyama (1985) demonstrated in heating experiments that such dusty zones formed by melting of sodic portions of plagioclase, and that the formation reflects a compositional adjustment of plagioclase at higher temperatures. The remaining plagioclase is more calcic, thus closer to equilibrium with the host melt at higher temperatures. This interpretation fits well for the dusty zones in Pinatubo samples, as tubal glass inclusions in the dusty zones are sodic compositions.

Thin calcic overgrowths surround the dusty zones and partially resorbed interiors of plagioclase phenocrysts, which indicates a period of cooling followed the heating event. Identical compositions of microlites in the groundmass and the rims of plagioclase phenocrysts indicate crystallization of microlites during the cooling. The rim compositions suggest an increase in MgO (2.5–3.5 wt%) and $Fe_2O_3^T$ (2.0–2.7 wt%) in the melt. Simultaneous increases in Ca, Fe, and Mg in the rims require incorporation of a mafic melt into the felsic magma chamber.

The dome extrusion started on June 7, 1991, and was followed by a discharge of vesiculated andesitic scoria on June 11–12 (Hoblitt et al. 1991). Subsequently, the dome was ejected together with dacitic pumice during the cataclysmic eruption on June 15, 1991. The June 11–12 scoria and June 7–15 dome-forming andesite have identical bulk compositions and mineral assemblages, and both contain rounded basalt inclusions, although the scoria does not contain plagioclase microlites or prominent overgrowths (Rutherford et al. 1993; Pallister et al. 1996). The similar compositions of the two have been taken to indicate the same mixed magma source (Rutherford et al. 1993; Pallister et al. 1996), which implies that the nucleation of microlites and overgrowth of phenocrysts in the dome-forming andesite took place during the short period of its extrusion, approximately several days. This conclusion is in accord with inhomogeneous compositions of oxides in the andesite (Pallister et al. 1996) because oxides could be equilibrated within several days at magmatic temperatures (Hammond and Taylor 1982).

Hot mafic melt that injected into a cool felsic magma likely released volatiles, producing a gas-charged mixed magma. This buoyant, mixed magma erupted as highly vesiculated andesite scoria. A portion of the mixed magma, which slowly lost volatiles, formed the viscous, dense, dome-forming andesite. Degassing of the mixed magma cooled the magma and lowered the melt H_2O, which raised the liquidus temperature of plagioclase and promoted the nucleation of microlites in the groundmass and the development of overgrowths on partially resorbed phenocrysts. This is supported by K_2O geothermometry of the rims and microlites (Fig. 7), which indicates their crystallization at a hotter temperature than the dacitic melt but a much cooler temperature than the mafic magma. K_2O contents of the outermost rims are similar to those of the interiors of plagioclase phenocrysts, suggesting the final temperature of the dome was similar to that of the dacitic magma, ~800 °C.

Magmas for dacitic pumice

Unlike the dome-forming andesite, plagioclase phenocrysts in white pumice do show neither prominent overgrowth of calcic rims nor plagioclase microlites. Partial resorption of the outermost edge of plagioclase is present but not observed in all grains. The lack of extensive resorption of plagioclase may be attributed to the large magma chamber. A seismic survey by Mori et al. (1993, 1996) indicated an irregularly shaped, laterally extensive magma body of 40–90 km^3 beneath Mount Pinatubo. Heating of such a large magma chamber would have been uneven, and the magma close to the mafic melt would have been subjected to more resorption than that in distal parts. Resorption textures are common in some gray pumice samples and especially in the gray bands of banded pumice, which show alternating layers of several millimeters to centimeter wide white and gray pumice. The pumice probably represents a portion of felsic magma closer to the mafic melt.

If the incursion of a mafic melt into upper crustal level took place long before the eruption, the surface of resorbed plagioclase should have been healed by accretion of plagioclase. The lack of overgrowths on these plagioclase phenocrysts indicates the short time span between the heating by a mafic melt and the eruption.

The outer margins of some phenocrysts show a slight increase in $Fe_2O_3^T$ without increase in MgO. Incorporation of a mafic melt is not a possible cause because of low MgO and CaO in the phenocrysts. We conclude that oxidation of the magma increased the ratio of $Fe^{3+}/\Sigma Fe$ and consequently the content of $Fe_2O_3^T$ in plagioclase. This interpretation is consistent with progressive oxidation of the felsic magma as proposed in a study of sulfur-bearing phases in the dacitic pumice (Hattori 1993, 1996).

Oscillatory zoning in the interior of plagioclase phenocrysts

Variation in An contents of plagioclase phenocrysts may be caused by repeated injections of mafic melts, a fluctuation of total pressure, diffusion-crystallization kinetics, a fluctuation of temperature, or a variation in H_2O of the magma.

Recurrent injections of mafic magma. Recurrent injections of mafic magma have been suggested as a possible cause of Ca spikes in plagioclase phenocrysts (e.g., Luhr and Melson 1996), but this would produce high Mg^{2+} and Fe^{3+} in the calcic zones of plagioclase. This possibility is rejected because of low and consistent $Fe_2O_3^T$ and MgO in the interiors of plagioclase.

A change in total pressure. A change in total pressure has a minor effect on Ca^{2+} and Na^+ contents of plagioclase, and this factor is discounted as the major cause of the fluctuations in An. For example, the loop shape of liquidus and solidus curves in the binary system of anorthite-albite at 1 atm is not much different from that at 5 kbar, indicating the trivial effect of pressure on plagioclase compositions (Yoder et al. 1957). Furthermore, this is not supported by consistent Al^{3+} contents of hornblende indicating a depth of ~10 km (Rutherford et al. 1993).

Diffusion-crystallization kinetics. Slower diffusion of Ca^{2+} and Al^{3+} than of Na^+ and Si^{4+} in melts may yield compositional gradients in the melt near plagioclase surfaces, producing oscillatory zoning (e.g., L'Heureux and Fowler 1994). This is, however, discounted as a significant cause of zoning in the Pinatubo samples because the observed zoning is commonly accompanied by resorption of inner Na-rich portions, which cannot be explained by the model. In addition, the observed pattern, gradual decrease in An toward the rims, contrasts with the pattern expected from the model because a greater diffusion rate for Na^+ than for Ca^{2+} in a melt would produce a pattern with a gradual increase in Ca^{2+} toward the rim followed by a sharp drop of Ca^{2+} (L'Heureux 1993; L'Heureux and Fowler 1994).

Fluctuation of temperatures. Fluctuations in temperatures may be produced by magma convection. High crys-

tallinity (~55 vol%), cool temperatures (~800 °C), and high SiO_2 of the Pinatubo magma do not appear favorable for its thermal convection, but these adverse factors could be outweighed by its high H_2O contents (<4.4 wt%, Westrich and Gerlach 1992; 6.1–6.6 wt%, Wallace 1993). Granitic magma at 800 °C and saturated with H_2O at a depth of 10 km, has a viscosity of $10^{4.5-5}$ poise, which is similar to the viscosity of dry basaltic melt at 1000 °C at a similar depth (Persikov 1991). Other volatiles, such as CO_2 and F, further lowered the melt viscosity. In addition, a thick (>100 m) magma chamber, like the Pinatubo magma chamber, is expected to have convection (Marsh 1988) because Rayleigh number (Ra) is a function of the cube of layer thickness (L); $Ra = (\alpha g \Delta T L^3)/\nu\kappa$, where α is the coefficient of thermal expansion (5×10^{-5} K^{-1}), g is the gravitational constant (980.7 cm/s^2), ΔT is the temperature difference (100 K), ν is kinematic viscosity (10^5 poise), and κ is thermal diffusivity (10^{-2} cm^2/s). The Ra value for the preeruptive magma chamber of 1 km thickness is calculated to be $\sim 7 \times 10^3$, which warrants vigorous convection. The thickness of 1 km is reasonable, considering the large amount (~2.5–4 km^3 as a dense mass) of magma discharged during a 12 h period, the lack of nonjuvenile materials in the eruption products, and the huge volume of magma remaining beneath Mount Pinatubo after the eruption (Mori et al. 1993, 1996).

In a viscous magma, a crystal with density similar to the melt would flow with a melt without sinking (Marsh 1988). Settling speed (V) in a crystal-free melt may be expressed by Stokes' law: $V = 2/9 g \Delta\rho r^2/\eta$, where $\Delta\rho$ is density contrast, r is radius of crystals, and η is melt viscosity. For the Pinatubo magma at 800 °C, a depth of 10 km, and a density of 2.09–2.15 g/cm^3 [calculated using the matrix glass compositions in Table 1, and partial molar volumes, thermal expansions, compressibility of oxides, and zero partial molar volume of H_2O given by Lange and Carmichael (1987) and Lange (1994)], the settling velocity of 1 mm spherical plagioclase (An_{40-80}) with a density of 2.61–2.67 g/cm^3 (calculated using the density and thermal expansion rates by Smith and Brown 1988) is very small, $\sim 1.1 \times 10^{-3}$ cm/s (~14 m/yr). Plagioclase likely traveled together with a melt in a convective cell. Plagioclase would accrete more sodic compositions during its upward flow and undergo partial resorption during its downward flow. The variation of An_{35-50} could be formed from a convection magma with 4 wt% H_2O at temperatures ranging from 800 to 860 °C (calculated using equations by Housh and Luhr 1991).

Thermal convection of a magma may be enhanced by degassing as it amplifies the density difference of the melt, although the difference in H_2O in the melt at the depth of 10 km is very small. A water-saturated, 1 km thick magma would lose <0.1 wt% H_2O during upward flow (using the solubility of H_2O by Burnham 1979, 1994). Nevertheless, the degassing would amplify the variation in An because plagioclase formed from a melt with lower H_2O would contain lower An.

The convection of the parent magma is supported by the huge volume of magma with relatively homogeneous compositions (~64 wt% SiO_2), similar textures, and even distribution of crystals throughout the eruption products. The magma, however, likely became stagnant before eruption owing to high crystallinity (>55 vol%) judging from angular, delicately shaped sulfides in groundmass glass (Hattori 1993, 1996), different compositions of the outermost rims of plagioclase phenocrysts (Luhr and Melson 1996; this study), heterogeneous glass compositions (Westrich and Gerlach 1992; Pallister et al. 1996), and different degrees of resorption of plagioclase phenocrysts in the eruption products.

Fluctuation of H_2O. Plagioclase with An_{35-50} can be formed at a constant temperature from a melt containing 3.1 to 5.4 wt% H_2O (calculated using the matrix-glass composition of Ca/Na molar ratio = 0.214, Table 1, and the Ca-Na exchange-reaction constant given by Sisson and Grove 1993). The H_2O contents are within the range observed in melt inclusions [1.3–4.4 wt%, Westrich and Gerlach (1992); 6.1–6.6 wt%, Wallace (1993); 6.4 wt%, Rutherford et al. (1993)]. As described above, such a change in H_2O cannot be generated in a 1 km thick convective cell, but introduction of external fluids, such as meteoric waters and fluids originating from underlying mafic magmas, may yield a variation in melt H_2O. Meteoric waters may be incorporated into shallow crustal magma chambers either directly or through assimilation of altered rocks (e.g., Hattori and Muehlenbachs 1982; Hildreth et al. 1984; Larson and Geist 1995). This is supported by $^3He/^4He$ ratios lower than atmospheric He for inclusions in a plagioclase phenocryst (B. Marty and K. Hattori, unpublished data). Mafic magmas intruding beneath Mount Pinatubo would also contribute to a fluctuation in the H_2O in the overlying felsic magma. Mafic magmas discharge varying compositions of volatiles during their ascent and solidification. For example, CO_2 originating from a mafic magma would pass through the overlying felsic magma because of its low solubility in a melt. The CO_2 would drain H_2O from the felsic magma because of mutual solubility of the two gases (e.g., Holloway 1976). Volatiles and bubbles move very slowly in a viscous silicate melt, but they can be effectively transported in a convecting magma chamber (e.g., Shinohara et al. 1995).

The proposed interpretation is supported by deep (~30 km) seismic activity caused by sudden fluid movement beneath Mount Pinatubo (Harlow et al. 1996). Second, fluctuation in melt H_2O is postulated from variable H_2O contents in melt inclusions (Westrich and Gerlach 1992; Rutherford et al. 1993) and variable CO_2/H_2O in melt inclusions (Wallace 1993) and fluid inclusions in phenocrysts (Harris et al. 1993). Third, this interpretation is consistent with the presence of high spikes of Ca (An = ~80) in the interiors of plagioclase phenocrysts. The Ca spikes are not accompanied by high Mg and Fe but are commonly accompanied by prominent corrosion of inner growth zoning. They could not have formed by temperature fluctuations in a convection cell. Such spikes prob-

ably formed by periodic incorporation of large quantities of hot fluids, which likely originated from underlying mafic magmas.

Acknowledgments

K.H. thanks Raymond S. Punongbayan and Christopher G. Newhall for assisting the author's field work, Ron Hartree for XRF analysis, and Peter Jones for SEM analysis. H.S. is grateful to A. Minami for electron probe assistance. The authors acknowledge helpful comments by Cel Collins, J. Al Donaldson, Ivan L'Heureux, Malcolm J. Rutherford, Ralph Kretz, and John Stix, and the reviews of James F. Luhr, John S. Pallister, and Brad S. Singer. This project was supported by National Sciences and Engineering Research Council of Canada grants to K.H. and a Grant-in-Aid for Scientific Research from the Ministry of Education, Science and Culture of Japan, to H.S.

References cited

Baschek, G., and Johannes, W. (1995) The estimation of NaSi-CaAl interdiffusion rates in peristerite by homogenization experiments. European Journal of Mineralogy, 7, 295–307.

Beattie, P., Drake, M., Jones, J., Leeman, W., Longhi, J., McKay, G., Nielsen, R., Palme, H., Shaw, D., Takahashi, E., and Watson, B. (1993) Terminology for trace-element partitioning. Geochimica et Cosmochimica Acta, 57, 1605–1606.

Bernard, A., Knittel, U., Weber, B., Weis, D., Albrecht, A., Hattori, K., Klein, J., and Oles, D. (1996) Petrology and geochemistry of the 1991 eruption products of Mt. Pinatubo. In R.S. Punongbayan and C.G. Newhall, Eds., Fire and mud eruptions and lahars of Mount Pinatubo, Philippines, p. 767–797. University of Washington Press, Seattle.

Blundy, J., and Wood, B. (1994) Prediction of crystal-melt partition coefficients from elastic module. Nature, 372, 452–454.

Bluth, G.J.S., Doiron, S.D., Schnetzler, C.C., Krueger, A.J., and Walter, L.S. (1992) Global tracking of the SO_2 clouds from the June, 1991 Mount Pinatubo eruptions. Geophysical Research Letters, 19, 151–154.

Burnham, C.W. (1979) The importance of volatile constituents. In H.S. Yoder, Ed., The evolution of the igneous rocks: Fiftieth anniversary perspectives, p. 439–482. Princeton University Press, New Jersey.

——— (1994) Development of the Burnham model for prediction of H_2O solubility in magmas. In Mineralogical Society of America Reviews in Mineralogy, 30, 123–129.

Dingwell, D.B., Brearley, M., and Dickinson, J.E., Jr. (1988) Melt densities in the Na_2O-FeO-Fe_2O_3-SiO_2 system and the partial molar volume of tetrahedrally-coordinated ferric iron in silicate melts. Geochimica et Cosmochimica Acta, 52, 2467–2475.

Drake, M.J. (1976) Plagioclase-melt equilibria. Geochimica et Cosmochimica Acta, 40, 457–466.

Grove, T.L, Baker, M.B., and Kinzler, R.J. (1984) Coupled CaAl-NaSi diffusion in plagioclase feldspar: Experiments and application to cooling rate speedometry. Geochimica et Cosmochimica Acta, 48, 2113–2121.

Hammond, P.A., and Taylor, L.A. (1982) The ilmenite/titano-magnetite assemblage: Kinetics of re-equilibration. Earth and Planetary Science Letters, 61, 143–150.

Harlow, D.H., Power, J.A., Laguerta, E.P., Ambubuyog, G., White, R.A., and Hoblitt, R.P. (1996) Precursory seismicity and forecasting of the June 15, 1991, eruption of Mount Pinatubo. In R.S. Punongbayan and C.G. Newhall, Eds., Fire and mud eruptions and lahars of Mount Pinatubo, Philippines, p. 285–305. University of Washington Press, Seattle.

Harris, T.N., Wopenka, B., Pasteris, J.D., and Wang, A. (1993) A Raman microprobe study of fluid and solid inclusions in quartz phenocrysts from pyroclastic flow deposits of the Mount Pinatubo eruption: Another attempt to account for "missing" SO_2. Abstracts with Programs, Annual Geological Society of America, 25, A-43.

Hattori, K. (1993) High-sulfur magma, a product of fluid discharge from underlying mafic magma: Evidence from Mount Pinatubo, Philippines. Geology, 21, 1083–1086.

——— (1996) Occurrence of sulfide and sulfate in the 1991 Pinatubo eruption products and their origin. In R.S. Punongbayan and C.G. Newhall, Eds., Fire and mud eruptions and lahars of Mount Pinatubo, Philippines, p. 807–824. University of Washington Press, Seattle.

Hattori, K., and Muehlenbachs, K. (1982) Oxygen isotope ratios of the Icelandic crust. Journal of Geophysical Research, 87, 6559–6565.

Hildreth, W., Christiansen, R.L., and O'Neil, J.R. (1984) Catastrophic isotopic modification of rhyolitic magma at times of caldera subsidence, Yellowstone Plateau volcanic field. Journal of Geophysical Research, 89, 8339–8369.

Hoblitt, R.P., Wolfe, E.W., Lockhart, A.B., Murray, T.L., Harlow, D.H., Mori, J., Daag, A.S., and Tubianosa, B.S. (1991) 1991 eruptive behavior of Mount Pinatubo, Philippines. Eos, 72(44), 61.

Holloway, J.R. (1976) Fluids in the evolution of granitic magmas: Consequences of finite CO_2 solubility. Geological Society of America Bulletin, 87, 1513–1518.

Housh, T.B., and Luhr, J.F. (1991) Plagioclase-melt equilibria in hydrous systems. American Mineralogist, 76, 477–492.

Jensen, B.B. (1973) Patterns of trace element partitioning. Geochimica et Cosmochimica Acta, 37, 2227–2242.

Johannes, W. (1978) Melting of plagioclase in the system Ab-An-H_2O and Qz-Ab-An-H_2O at f_{H_2O} = 5 kbars, an equilibrium problem. Contributions to Mineralogy and Petrology, 66, 295–303.

Knittel, U., Hattori, K., Hoefs, J., and Oles, D. (1992) Isotopic compositions of anhydrite phenocryst-bearing pumices from the 1991 eruption of Mount Pinatubo, Philippines. Eos, 73, 342.

Kudo, A.M., and Weill, D.F. (1970) An igneous plagioclase thermometer. Contributions to Mineralogy and Petrology, 25, 52–62.

Lange, R.A. (1994) The effect of H_2O, CO_2, and F on the density and viscosity of silicate melts. In Mineralogical Society of America Reviews in Mineralogy, 30, 331–369.

Lange, R.A., and Carmichael, I.S.E. (1987) Densities of Na_2O-K_2O-CaO-MgO-FeO-Fe_2O_3-Al_2O_3-TiO_2-SiO_2 liquids: New measurements and derived partial molar properties. Geochimica et Cosmochimica Acta, 51, 2931–2946.

Larson, P.B., and Geist, D.J. (1995) On the origin of low-^{18}O magmas: Evidence from the Casto pluton, Idaho. Geology, 23, 909–912.

L'Heureux, I. (1993) Oscillatory zoning in crystal growth: A constitutional undercooling mechanism. Physical Review E, 48, 4460–4469.

L'Heureux, I., and Fowler, A.D. (1994) A nonlinear dynamical model of oscillatory zoning in plagioclase. American Mineralogist, 79, 885–891.

Longhi, J., Walker, D., and Hays, J.F. (1976) Fe and Mg in plagioclase. Proceedings of the Lunar Science Conference, 7, 1281–1300.

Loomis, T.P. (1979) An empirical model for plagioclase equilibrium in hydrous melts. Geochimica et Cosmochimica Acta, 43, 1753–1759.

Luhr, J.F., and Melson, W.G. (1996) Mineral and glass compositions in June 15, 1991, pumices: Evidence for dynamic disequilibrium in the Pinatubo dacite. In R.S. Punongbayan and C.G. Newhall, Eds., Fire and mud eruptions and lahars of Mount Pinatubo, Philippines, p. 733–750. University of Washington Press, Seattle.

Marsh, B.D. (1988) Crystal capture, sorting, and retention in convecting magma. Bulletin of the Geological Society of America, 100, 1720–1737.

Marsh, B.D., Fournelle, J., Myers, J.D., and Chou, I-M. (1990) On plagioclase thermometry in island arc rocks: Experiments and theory. In R.J. Spencer and I-M. Chou, Eds., Fluid-mineral interactions. Geochemical Society Special Publication, 2, 65–83.

Matsui, Y., Onuma, N., Nagasawa, H., Higuchi, H., and Banno, S. (1977) Crystal structure control in trace element partition between crystal and magma. Bulletin de la Société français de Minéralogie et de Cristallographie, 100, 315–324.

McGee, J.J. (1993) Lunar ferroan anorthosites: Mineralogy, compositional variations and petrogenesis. Journal of Geophysical Research, 98, 9089–9105.

Möller, P. (1988) The dependence of partition coefficients on differences of ionic volumes in crystal-melt systems. Contributions to Mineralogy and Petrology, 99, 62–69.

Mori, J., Eberhart-Phillips, D., and Harlow, D. (1993) 3-dimensional velocity structure at Mount Pinatubo, Philippines: Resolution of magma bodies and earthquake hypocenters. Eos, 74(43), 667.

——— (1996) Three-dimensional velocity structure at Mount Pinatubo, Philippines: Resolving magma bodies and earthquake hypocenters. In R.S. Punongbayan and C.G. Newhall, Eds., Fire and mud eruptions and lahars of Mount Pinatubo, Philippines, p. 371–382. University of Washington Press, Seattle.

Mysen, B.O. (1988) Structure and properties of silicate melts, 354 p. Elsevier, New York.

Onuma, N., Higuchi, H., Wakita, H., and Nagasawa, H. (1968) Trace element partition between two pyroxenes and the host lava. Earth and Planetary Science Letters, 5, 47–51.

Pallister, J.S., Hoblitt, R.P., and Reyes, A.G. (1992) A basalt trigger for the 1991 eruptions of Pinatubo volcano? Nature, 356, 426–428.

Pallister, J.S., Hoblitt, R.P., Meeker, G.P., Knight, R.J., and Siems, D.F. (1996) Magma mixing at Mount Pinatubo: Petrographic and chemical evidence from the 1991 deposits. In R.S. Punongbayan and C.G. Newhall, Eds., Fire and mud eruptions and lahars of Mount Pinatubo, Philippines, p. 687–731. University of Washington Press, Seattle.

Persikov, E.S. (1991) The viscosity of magmatic liquids: Experiment, generalized patterns, a model for calculation and prediction: Applications. In L.L. Perchuk and I. Kushiro, Eds., Physical chemistry of magma, p. 1–40. Springer-Verlag, New York.

Phinney, W.C. (1992) Partition coefficients for iron between plagioclase and basalt as a function of oxygen fugacity: Implications for Archean and lunar anorthosites. Geochimica et Cosmochimica Acta, 56, 1885–1895.

Rutherford, M.J. (1993) Experimental petrology applied to volcanic processes. Eos, 74, 49 and 55.

Rutherford, M.J., Baker, L., and Pallister, J.S. (1993) Petrologic constraints on timing of magmatic processes in the 1991 Pinatubo volcanic system. Eos, 74(43), 671.

Sack, R.O., Carmichael, I.S.E, Rivers, M., and Ghiorso, M.S. (1980) Ferric-ferrous equilibria in natural silicate liquids at 1 bar. Contributions to Mineralogy and Petrology, 75, 369–376.

Sato, H. (1984) Partition relation of K between magma and plagioclase in a suite of volcanic rocks from northeast Shikoku, Japan. Journal of the Japanese Association of Mineralogists, Petrologists and Economic Geologists, 79, 47–59.

——— (1989) Mg-Fe partitioning between plagioclase and liquid in basalts of Hole 504B, Leg 111: A study of melting at 1 atm. Proceedings of Ocean Drilling Program, Scientific Results, 111, 17–26.

Sato, H., Hattori, K., and Nakada, S. (1993) Contrasting styles of magma interaction at Unzen and Pinatubo: Evidence from zoning of plagioclase. Eos, 74(43), 671.

Scott, W.E., Hoblitt, R.P., Torres, R.C., Self, S., Martinez, M.L., and Nillos, T., Jr. (1996) Pyroclastic flows of the June 15, 1991, climactic eruption of Mount Pinatubo. In R.S. Punongbayan and C.G. Newhall, Eds., Fire and mud eruptions and lahars of Mount Pinatubo, Philippines, p. 545–570. University of Washington Press, Seattle.

Shinohara, H., Kazahaya, K., and Lowenstern, J.B. (1995) Volatile transport in a convecting magma column: Implications for porphyry Mo mineralization. Geology, 23, 1091–1094.

Singer, B.S., Dungan, M.A., and Layne, G.D. (1995) Textures and Sr, Ba, Mg, Fe, K, and Ti compositional profiles in volcanic plagioclase: Clues to the dynamics of calc-alkaline magma chambers. American Mineralogist, 80, 776–798.

Sisson, T.W., and Grove, T.L. (1993) Experimental investigations of the role of H_2O in calc-alkaline differentiation and subduction zone magmatism. Contributions to Mineralogy and Petrology, 113, 143–166.

Smith, J.V., and Brown, W.L. (1988) Feldspar minerals: 1. Crystal structures, physical, chemical, and microtextural properties (2nd edition), 828 p. Springer-Verlag, New York.

Tsuchiyama, A. (1985) Dissolution kinetics of plagioclase in melt of the system diopside-albite-anorthite and the origin of dusty plagioclase in andesites. Contributions to Mineralogy and Petrology, 89, 1–16.

Wallace, P. (1993) Pre-eruptive gas saturation in the June 15, 1991, Mount Pinatubo Dacite: New evidence from CO_2 contents of melt inclusions. Eos, 74(43), 668.

Weill, D.F., Hon, R., and Navrotsky, A. (1980) The igneous system $CaMgSi_2O_6$-$CaAl_2Si_2O_8$-$NaAlSi_3O_8$: Variations on a classic theme by Bowen. In B. Hargraves, Ed., Physics of magmatic processes, p. 49–92. Princeton University Press, New Jersey.

Westrich, H.R., and Gerlach, T.M. (1992) Magmatic gas source for the stratospheric SO_2 cloud from the June 15, 1991, eruption of Mount Pinatubo. Geology, 20, 867–870.

Yoder, H.S., Stewart, D.B., and Smith, J.R. (1957) Ternary feldspars. Carnegie Institution of Washington Year Book, 56, 206–214.

Manuscript received April 20, 1995
Manuscript accepted March 20, 1996